JOURNAL OF GEOPHYSICAL RESEARCH, VOL. 114, E11007, doi:10.1029/2009JE003355, 2009

Click Here for Full Article

The effect of salt crust on the thermal conductivity of one sample of fluvial particulate materials under Martian atmospheric pressures

Marsha A. Presley,[1] Robert A. Craddock,[2] and Natalya Zolotova[3]

Received 2 February 2009; revised 13 July 2009; accepted 24 July 2009; published 7 November 2009.

[1] A line-heat source apparatus was used to measure thermal conductivities of a lightly cemented fluvial sediment (salinity = 1.1 g · kg^{-1}), and the same sample with the cement bonds almost completely disrupted, under low pressure, carbon dioxide atmospheres. The thermal conductivities of the cemented sample were approximately 3× higher, over the range of atmospheric pressures tested, than the thermal conductivities of the same sample after the cement bonds were broken. A thermal conductivity-derived particle size was determined for each sample by comparing these thermal conductivity measurements to previous data that demonstrated the dependence of thermal conductivity on particle size. Actual particle-size distributions were determined via physical separation through brass sieves. When uncemented, 87% of the particles were less than 125 μm in diameter, with 60% of the sample being less than 63 μm in diameter. As much as 35% of the cemented sample was composed of conglomerate particles with diameters greater than 500 μm. The thermal conductivities of the cemented sample were most similar to those of 500-μm glass beads, whereas the thermal conductivities of the uncemented sample were most similar to those of 75-μm glass beads. This study demonstrates that even a small amount of salt cement can significantly increase the thermal conductivity of particulate materials, as predicted by thermal modeling estimates by previous investigators.

Citation: Presley, M. A., R. A. Craddock, and N. Zolotova (2009), The effect of salt crust on the thermal conductivity of one sample of fluvial particulate materials under Martian atmospheric pressures, *J. Geophys. Res.*, *114*, E11007, doi:10.1029/2009JE003355.

1. Introduction

[2] Salt crusts have been observed at the Viking Lander sites [*Binder et al.*, 1977; *Mutch et al.*, 1976], the Pathfinder landing site [*Rieder et al.*, 1997; *Moore et al.*, 1999], and by both Mars Exploration Rovers (MER) [*Squyres et al.*, 2004; *Gellert et al.*, 2004]. Crusted particulates were first observed on the Martian surface near the Viking 1 spacecraft where overlying sediment had been swept clear by retrorocket exhaust (Figure 1). Polygonal fractures within this material indicate a degree of cohesiveness that is not present in loose, unindurated particulates. Cohesive "clods" obtained by the Viking Landers' sampling arms would break up completely when the samples were sieved [*Clark et al.*, 1976]. Such friability suggests that the material was only lightly cemented.

[3] Building on the data from the surface, investigation of spacecraft data from the Viking Infrared Thermal Mapper (IRTM) and the Mars Global Surveyor Thermal Emission Spectrometer (TES) revealed large regional areas of intermediate albedo and thermal inertia that have been interpreted to be indurated particulate materials [*Kieffer et al.*, 1981; *Jakosky and Christensen*, 1986; *Presley and Arvidson*, 1988; *Christensen and Moore*, 1992; *Merényi et al.*, 1996; *Mellon et al.*, 2000; *Putzig et al.*, 2005]. Each of these studies assumed that a cementing agent within the pores of the material would increase the thermal conductivity, and therefore the thermal inertia, of particulate materials, but the magnitude of such an effect was unknown. While thermal conductivity models have been developed that include the effects of ice [e.g., *DeVries*, 1952; *Johansen*, 1975], including under Martian atmospheric conditions [*Mellon et al.*, 1997], thermal conductivity modeling efforts specifically concerning salts under Martian atmospheres have only recently been published [*Mellon et al.*, 2008; *Piqueux and Christensen*, 2009]. Similarly, there have been only a few laboratory studies on the influence of salt-cements on thermal conductivity, with none performed under Martian conditions.

[4] Under terrestrial atmospheric conditions, *Abu-Hamdeh and Reeder* [2000] measured a *decrease* in thermal conductivity with increasing salt concentration when the salt was added to the soil as an aqueous solution. In the current Martian environment, however, *liquid* aqueous solutions will not be a factor at the surface. *Van Rooyen and*

[1]School of Earth and Space Exploration, Mars Space Flight Facility, Arizona State University, Tempe, Arizona, USA.
[2]Center for Earth and Planetary Studies, National Air and Space Museum, Smithsonian Institution, Washington, DC, USA.
[3]School of Earth and Space Exploration, Arizona State University, Tempe, Arizona, USA.

Copyright 2009 by the American Geophysical Union.
0148-0227/09/2009JE003355$09.00

Figure 1. An example of a crusted material on the Martian surface. The image is a portion of Viking Lander image 12A136, where the retrorocket exhaust had swept the surface clear of overlying sediment. The polygonal fractures indicate a degree of cohesiveness that is not present in loose, unindurated particulates.

Winterkorn [1959], in contrast, find that under terrestrial conditions the thermal conductivity of salt-cemented sand in a "nearly dry" state was indeed higher than that of salt-free sand. Similarly, *Seiferlin et al.* [2007] measured an increase in thermal conductivity, under a vacuum, using wax as a cementing agent between small glass beads. Moreover, they observed an increase in thermal conductivity with an increase in the amount of "cement." The effect of salt cementation under Martian atmospheric pressures, however, has yet to be investigated in the laboratory.

[5] *Mellon et al.* [2008] and *Piqueux and Christensen* [2009] have recently modeled the thermal effects of salt-cement in the pore spaces between particulates under Martian atmospheric pressures. Both studies indicated that minute quantities of salt cement could have profound effects on the bulk thermal conductivity of particulate materials. *Mellon et al.* [2008] report that 1% by volume of a cementing agent could increase the thermal conductivity by 5 to 50 times. *Piqueux and Christensen* [2009] report that cement fractions of 0.001% to 1% by volume will increase the thermal conductivity by a factor of 3 to 8 times. From 1 to 15% cement by volume the increase in thermal conductivity is 20–50%, with thermal conductivity values rapidly increasing to that of rock for fractions greater than 15% by volume.

[6] An ideal study of the effect of salt-cementation on the thermal conductivity of particulate materials would include three components: a laboratory component in which the amount and type of cement and atmospheric pressure are systematically varied, a field component in which naturally occurring cemented particulate deposits are investigated, and a theoretical component to aid the interpretation of the experimental and field measurements. The laboratory component increases our understanding of how variations in physical characteristics affect the thermal conductivity of particulate materials, and what the magnitude of those changes are going to be. A theoretical component helps interpret these effects, and laboratory results in turn can lead to more accurate thermal conductivity models. The field component increases our understanding of the geological and environmental contexts in which these thermophysical variations occur. Together these components would improve our ability to interpret variations in the surface temperature data in terms of the geology of the planetary surface.

[7] Yet the difficulties associated with measuring the effect of salt crusts/cement on thermal conductivity are numerous. Sampling a crusted sediment for measurement back in the lab will break the salt bonds, particularly in a friable, lightly cemented sediment. Transportation, particularly over long distances, is likely to disrupt the cement bonds even further. The use of a thermal conductivity probe, whether in a lab or in situ, would break the salt bonds upon insertion into the indurated sediment and create a layer of disturbed soil around the probe. All of these effects would likely lower the thermal conductivity measured relative to the actual thermal conductivity.

[8] Formation of uniform samples of lightly indurated particulate materials, for in situ laboratory analysis, is also not an easy task. The texture and nature of the cement formed will depend on the formation conditions: the amount of water initially present, the composition and concentration of salts within the aqueous solution, and whether the solution evaporates or freezes and then sublimates [e.g., *Goodall et al.*, 2000]. Heterogeneity in the distribution and texture of the salt is an expected result and may bias thermal conductivity measurements. In order to avoid disruption of the cement, the line-heat source would need to be in place either prior to adding the aqueous solution to the sample or at least prior to evaporation of the solution. That sequence, however, increases the possibility that even a small amount of salt may form a bridge between the heating wire (or thermal conductivity probe) and the soil immediately adjacent to it. Such a bridge could bias thermal conductivity measurements to higher values than may be appropriate.

[9] While these limitations have hindered the development of a systematic study, the effect of induration on thermal conductivity under Martian atmospheric pressures has been measured for one naturally occurring fluvial sample. Although it is only one sample, under nonideal conditions, the results demonstrate that even a relatively small amount of cement will significantly increase the thermal conductivity.

2. Background

[10] Measurements taken by the Viking Landers' X-ray Fluorescence spectrometers indicated that the Martian surficial fines contained an abundance of sulfur [*Clark et al.*, 1976]. Initial geochemical interpretation of those chemical analyses suggested that the Martian surficial deposits contained 10–15% kieserite ($MgSO_4 \cdot H_2O$), 5–10% calcite ($CaCO_3$), and ~1% NaCl [*Baird et al.*, 1976]. *Burns* [1987, 1988] later argued that ferric sulfates of the copiapite and jarosite groups were also possible constituents of the Martian surface.

[11] From an orbital perspective, much of the Martian surface can be classified as low albedo, high thermal inertia regions, such as Syrtis Major and Sinus Meridiani, or as high albedo, low thermal inertia regions, such as Arabia and Tharsis. Western Arabia Terra (aka Oxia) is one example of a large region that does not fit that bimodal classification. While its thermal inertia (200 $J \cdot m^{-2} s^{-1/2} K^{-1}$) is intermediate between that of the bright areas (130 $J \cdot m^{-2}$

$s^{-1/2}$ K^{-1}) and that of the dark areas (240 J · m^{-2} $s^{-1/2}$ K^{-1}), its violet reflectance (0.05–0.06) is as low as the dark areas (0.05–0.065) and its red reflectance (0.14–0.17) is almost, but not quite, as bright as the bright areas (0.16–0.21) [*Presley and Arvidson*, 1988].

[12] When red and blue reflectances, derived from the Viking Orbiter camera data, were plotted on a two-dimensional histogram, a mixing trend between the dark violet (Sinus Meridiani) material and the bright red (Arabia) material was readily apparent, as was a mixing trend between the intermediate ("brown," Oxia) material and the bright red material [*Presley and Arvidson*, 1988, Figure 9]. In contrast, a clear mixing trend was not apparent between the dark violet end point material and the "brown" end point material, which suggested that the surface material in Oxia is relatively immobile [*Presley and Arvidson*, 1988].

[13] The thermal inertia of the material comprising Oxia averaged to about 200 J · m^{-2} $s^{-1/2}$ K^{-1} [*Presley and Arvidson*, 1988], which would correspond to a particle size in unindurated material of about 90 μm [*Presley and Christensen*, 1997]. On Mars, the threshold wind speed is at a minimum for a particle diameter of 115 μm [*Iversen and White*, 1982]. As such, the material comprising Oxia should be the most easily transported on Mars. Yet eolian bedforms are not visible in Viking images of this region [*Presley and Arvidson*, 1988]. Since the material appears to be immobile, an alternative explanation is that the surface material of Oxia is composed of a finer grain size that is lightly indurated [*Kieffer et al.*, 1981; *Jakosky and Christensen*, 1986; *Presley and Arvidson*, 1988].

[14] The color-albedo units characterized in the Oxia region are similar to those observed in the Chryse region (area of the Viking 1 Landing site) [*Merényi et al.*, 1996; *Arvidson et al.*, 1989]. *Mellon et al.* [2000] and *Putzig et al.* [2005] also included Oxia and Chryse in the same thermal inertia-albedo category. The similarity of thermal and optical properties with other regions suggests the possibility that crusted soils of similar properties may be widespread across the planet [e.g., *Jakosky and Christensen*, 1986].

[15] If Oxia and similar regions are composed of a salt-crusted material, logic suggests that the increased particle to particle connectivity must be balanced by an effective particle size that is much smaller than 90 μm in order to be consistent with the thermal data. One possibility then, is that these regions have a similar effective particle size as the bright red dust, in which case these regions would be indurated dust deposits.

[16] Most salts, including kieserite, however, exhibit no significant absorptions in the visible part of the spectrum. A "transparent" salt is therefore unlikely to specifically reduce the blue reflectance of the deposit. Iron sulfates such as quenstedtite [*Presley and Arvidson*, 1988] or jarosite [*Burns*, 1986, 1987, 1988; *Burns and Fisher*, 1990; *Burns*, 1993; *Presley*, 1995] are "trans-opaque," with absorption features in the blue end of the visible spectrum [*Hunt et al.*, 1971; *Bishop and Murad*, 2005], and could explain both the darkening and the loss of blue reflectance. Abundant jarosite has indeed been identified by the MER Opportunity [e.g., *Klingelhöfer et al.*, 2004; *Morris et al.*, 2006], in addition to simpler, transparent Mg and Ca sulfates [e.g., *Christensen et al.*, 2004; *Squyres et al.*, 2004; *Wang et al.*, 2006].

[17] Another surficial unit has since been identified that also has intermediate thermal inertia, but high albedo [*Putzig et al.*, 2005]. This unit has been interpreted as being a very thin deposit of dust that is thick enough to dominate the albedo, but thermally thin enough that it cannot mask the effects of a higher thermal inertia surface underneath [*Putzig et al.*, 2005]. Alternatively, this region could be an indurated deposit, but one with imperceptible amounts, if any, of trans-opaque salts.

[18] Although the theory that salt-cements are present over large regions of the surface seems to fit the data well, accurate interpretation is hindered by the scarcity of knowledge about the effect of salts on thermal properties under Martian conditions. The thermal conductivity measurements presented in this study present a small step toward clarification of the thermal effects of pore-filling cement.

3. Experimental Procedure

3.1. Sample

[19] The sample used for this study was a cemented, but very friable deposit collected from the Ross River floodplain east of the Simpson Desert in Australia [*Williams*, 1971; *Bourke and Pickup*, 1999; *Hollands et al.*, 2006]. The sample was obtained with a small core, approximately 8 cm in depth with a 2.5 cm radius. Prior to extraction, an area immediately adjacent to the sample location was measured in situ for bulk density and moisture content with a Model 3440 portable surface moisture density gauge manufactured by Troxler Electronic Laboratories. The moisture content affirmed that samples collected were dry (i.e., that it had not rained recently). The density measurements were to insure that the appropriate bulk density would be applied in the laboratory, as thermal conductivity may vary with bulk density [*Fountain and West*, 1970; M. A. Presley and P. R. Christensen, Thermal conductivity measurements of particulate materials: 4A. The effect of bulk density for granular particles, submitted to *Journal of Geophysical Research*, 2009].

[20] The sample was comprised of well-rounded particles, approximately 95% quartz, with minor amounts of potassium feldspar and just enough amorphous or microcrystalline hematite and goethite coating the grains to produce the red color characteristic of the Australian desert in that region [see *Hunter et al.*, 2006]. The salts forming the cement within the sample were expected to be dominated by typical evaporite salts including calcium carbonate, gypsum and potassium and sodium chlorides [e.g., *Lindsay*, 1987]. This expectation is consistent with the ion analysis discussed in section 3.4 (Table 1).

[21] The collection and transportation of the sample necessarily broke many of the cement bonds. When the sample was transferred into the sample holder for thermal conductivity measurement it had already taken the form of a mostly loose particulate material. Some of the sample was more highly indurated than other parts and the cement retained some identity through the formation of more durable clods. However, due to the small size of the sample holder, which is otherwise an advantage [*Presley and Christensen*, 1997], and due to the fragility of the platinum heating wire, clods larger than about 3 mm were removed ahead of time and not allowed in the sample holder.

Table 1. Concentration of Salt-Forming Ions Contained Within the Sample[a]

Ions	Concentration (mg/L)[b]	(mmol/g)[c]	(g/kg)[c]
Na^+	4.0	0.0009	0.020
NH_4^+	2.0	0.0005	0.010
K^+	22.4	0.0029	0.112
Mg^{2+}	8.0	0.0016	0.040
Ca^{2+}	20.3	0.0025	0.102
Subtotal		0.0126	0.283
Cl^-	4.6	0.0007	0.023
F^-	4.1	0.0011	0.020
NO_3^-	3.7	0.0003	0.018
SO_4^{2-}	8.4	0.0004	0.042
PO_4^-	1.0	0.0001	0.005
CO_3^{2-}	0.1	0.0000	0.000
HCO_3^-	143.9	0.0118	0.220
Subtotal		0.0148	0.719
Charge difference (Cation − anion molarities)		−0.0021	
Total Salinity (Sum of all ion concentrations)			1.112

[a]The values are averaged results from two samples.
[b]Concentrations are with respect to the volume of the deionized water used in the ion chromatography analysis.
[c]Concentrations are with respect to the weight of the soil sample.

[22] Once the thermal conductivity of the sample in this condition, referred to as the ''cemented sample,'' was measured, the sample was removed from the sample holder and the remaining cement bonds were broken by gently rubbing the sample by hand. A latex glove was used to avoid transferring oils, etc., onto the sample. The procedure was performed by hand so that the sediment particles themselves would not be broken and reduced in size. This state is referred to as the ''uncemented sample.''

3.2. Particle Size Analysis

[23] Particle size analyses were performed by physically separating the particles through brass sieves corresponding to Φ size intervals ($\Phi = -\log_2 d$, where d is the particle diameter in millimeters). One particle size analysis was performed prior to breaking the salt bonds, after the thermal conductivity of the cemented sample had been analyzed. The sieving was done by gently shaking the sieves by hand, in order to minimize further destruction of the cement bonds. After the bonds had been broken and the thermal conductivity of the uncemented sample had been evaluated, the sample was divided into two halves. Particle size analysis was performed on one half, using a RoTap to facilitate the sieving [see also *Presley and Christensen*, 1997; *Presley and Craddock*, 2006]. The other half was set aside for ion analysis.

3.3. Thermal Conductivity Measurements

[24] The line-heat source method was used to measure the thermal conductivity of the sample, due to its simplicity and proven reliability [*Cremers*, 1971; *Presley and Christensen*, 1997]. The laboratory set up was previously described in detail by *Presley and Christensen* [1997], with upgrades as discussed by *Presley and Craddock* [2006].

[25] A detailed error analysis and an assessment of accuracy of the thermal conductivities measured in this facility was presented by *Presley and Christensen* [1997, also submitted manuscript, 2009]. The typical precision of the thermal conductivity measurements is ±10%. For the lowest and highest values of the thermal conductivities measured in this study, the precision errors could reach ±20%.

[26] Measurements attained in this lab match those of *Smoluchowski* [1910], *Wechsler and Glaser* [1965], and *Hütter et al.* [2008], which are likely to be the most accurate thermal conductivity measurements previously obtained under Martian atmospheric pressures [*Presley and Christensen*, 1997, also submitted manuscript, 2009]. Furthermore, particle size estimates based on this laboratory's results and MER Rover thermal measurements match the particle size observed with the MER Rover Microscopic Imagers [*Fergason et al.*, 2006; *Hynek and Singer*, 2007]. Although there are no thermal conductivity ''standards'' available for comparison, these observations suggest that measurements obtained in this laboratory are reasonably accurate.

[27] The complete thermal conductivity data set is stored on Compact Disk. One copy is in the possession of the primary author. The other copy is stored at the Mars Space Flight Facility library at Arizona State University, Tempe, AZ, together with hard copies of abbreviated data files and a summary of the experimental conditions. Data are available upon request from the primary author.

3.4. Salinity

[28] In order to assess the amount of salt in the sample, the major cations and anions were analyzed by ion chromatography in E. Shock's GEOPIG laboratory at Arizona State University.

[29] After oven-drying the sample for 2 days, nanopure deionized water was added to the sample in a 5:1 ratio [e.g., *U.S. Salinity Laboratory Staff*, 1954], and the mixture was shaken for 2 hours. Since gypsum was a likely component of the salt [e.g., *Lindsay*, 1987] and takes longer to dissolve than most salts, the mixture was allowed to settle overnight in order to allow sufficient time for all of the salts to go into solution [e.g., *Schofield et al.*, 2001]. Salt-forming ions were then extracted from the sample by filtering the supernatant liquid through a 0.2 μm filter. The pH, carbonate and bicarbonate concentrations were determined via titration immediately after filtration [*Buurman et al.*, 1996]. The remaining solution was divided into two parts. The soluble anions were analyzed by anion-exchange chromatography (Dionex DX-600) using suppressed conductivity detection and a Dionex AS11 column. High-purity hydroxide eluent was generated by an on-line electrolytic eluent generator. Soluble cations were analyzed by suppressed conductivity detection using a Dionex Cation-Exchange CS12A column on a Dionex DX-120 chromatograph. Duplicates and blanks were run in each case to insure accuracy. Estimated analytical uncertainties for all ions are ±1% for this procedure.

4. Results

[30] The results of the ion analysis are presented in Table 1. The concentrations presented as mg $\cdot$ L^{-1} are the results from the ion chromatography analysis, and are with respect to the volume of deionized water used in the analysis. The concentrations presented as mmol $\cdot$ g^{-1}, are those results recalculated to be molar concentrations per

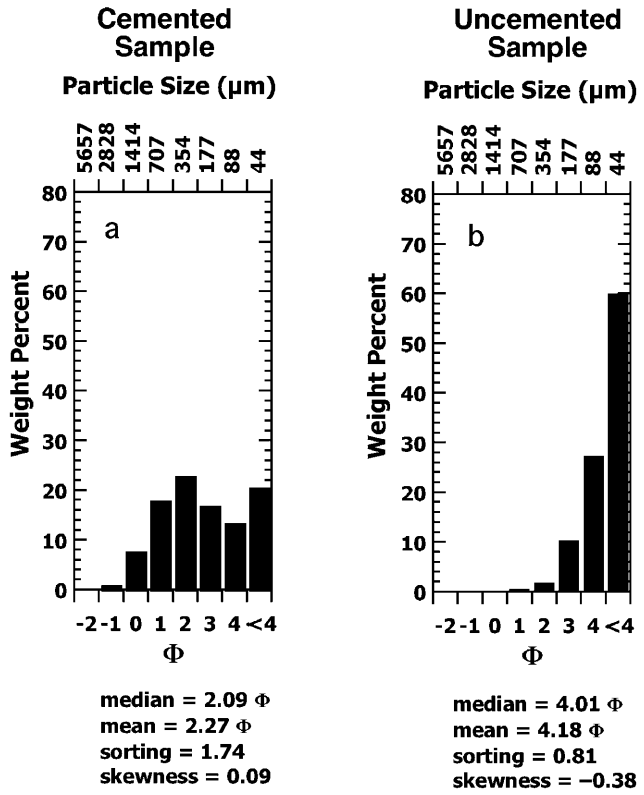

Figure 2. Particle sizes of the samples investigated in bins of Φ, where $\Phi = -\log d$, and plotted as histograms. The sample was collected from the Ross River floodplain, east of the Simpson Desert, Australia. (a) The particle size distribution of the sediment as sampled, with cement bonds broken only by the sampling process and transport. (b) The particle size distribution of the sample once the salt bonds have been broken as thoroughly as possible [results originally published by *Presley and Craddock*, 2006].

gram of soil. The difference between the total of the anion molar concentrations and the total of the cation molar concentrations is the charge imbalance. The resultant charge imbalance of −0.0021 is a relatively small difference and is likely an effect of averaging the results of two separate measurements, but also could be due to the presence of other non-salt-forming ions, minor amounts of salt-forming ions not analyzed for, and/or an intrinsic charge imbalance from the surface of the soil particles. The concentrations, presented as $g \cdot kg^{-1}$, are the ion chromatography results recalculated to be per kg of soil. The sum of the all of the concentrations of salt-forming ions in the sample is considered the salinity of the soil. A salinity of $1.1\ g \cdot kg^{-1}$ is consistent with the friability of the sample, and its lightly crusted appearance in situ.

[31] The particle size distributions are illustrated in Figure 2. Figure 2a represents the cemented sample, before the cement bonds were deliberately broken. The analysis is indicative of the sample as it was prepared for thermal conductivity measurement and not as it was *in situ*. As previously discussed, some of the cement bonds had been broken during collection and transport of the sample. Conglomerate particles larger than 2–3 mm were excluded from the sample due to the limitations of the thermal conductivity measurement. Figure 2b is the particle size distribution for the uncemented sample. Note that for both samples, the smallest sieve size used was 63 μm (4Φ). No attempt was made to further subdivide the <4Φ fraction. Hence the statistical parameters presented in Figure 2 are somewhat skewed by the likely incorrect assumption that all of the particles in the <4Φ fraction can be assigned as 5Φ (31–63 μm). Nonetheless, the cemented sample can be roughly described as a medium- to fine-grained sand, whereas, uncemented, the sample is more accurately described as a silt.

[32] The bulk density of the sediment measured in situ was $1600\ kg \cdot m^{-3}$. This packing density was the same as that measured for both cemented and uncemented forms when the sample was poured into the sample holder for thermal conductivity measurement. Hence no further adjustment was required to match the bulk density to that in the field.

[33] Figure 3 illustrates the thermal conductivities of (a) the cemented sample, and (b) those of the uncemented sample, measured over several atmospheric pressures from 0.5–20 torr (see also Table 2). For comparison purposes the thermal conductivity curves for 250–275 μm, 500–520 μm and 710–1000 μm glass beads [*Presley*, 1995] are included in Figure 3a, and the thermal conductivity curves for 25–30 μm, 70–75 μm and 90–100 μm glass beads [*Presley*, 1995] are included in Figure 3b.

5. Analysis

[34] As seen in Figure 2a, the thermal conductivities of the "cemented" fluvial sample are equivalent to those of an unindurated particle size of 500 μm. The thermal conductivities of the "uncemented" sample, after the salt bonds had been broken, match those of glass beads with a particle size of 70–75 μm (Figure 2b). These results are consistent with previous studies that indicate that the larger particle size fractions tend to control the thermal conductivity [*Presley and Craddock*, 2006; see also *Midttømme et al.*, 1997]. For these two samples, however, as much as 9% of the "cemented" sample is larger than 1000 μm, and at least 13% of the "uncemented" sample is larger than 75 μm. Particles larger than ~100 μm in both of these samples are likely to be conglomerate particles lightly held together with minimal cement, rather than individual solid grains.

6. Conclusions

[35] The thermal conductivities of the "cemented" sample are approximately 3× greater than the thermal conductivities of the "uncemented" sample. This experiment demonstrates that even in a lightly cemented sample where the cement bonds have been somewhat disrupted by the sampling process, salt cementation significantly increases the thermal conductivity.

[36] The result of this experiment should be considered a minimum effect that this amount of salt would have on the thermal conductivity, as unbroken cement bonds would undoubtedly contribute to an in situ thermal conductivity that would be higher than what was measured after sampling disrupted some of the cement bonding. Assuming a specific gravity of ~2.5 for the salt(s), a salinity value of

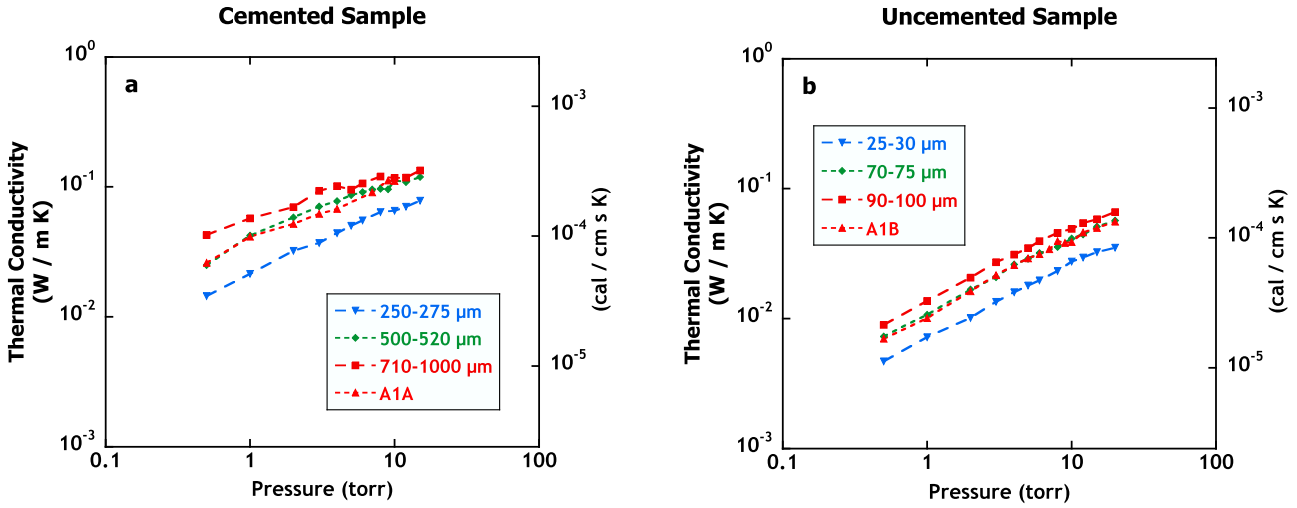

Figure 3. Plots of thermal conductivity versus atmospheric pressure for both the (a) cemented sample (A1A) and (b) the uncemented sample (A1B). Included in each plot are thermal conductivity data for glass beads [*Presley and Christensen*, 1997] of appropriate particle sizes for comparison. Thermal conductivities are presented here in SI units (W m^{-1} K^{-1}) on the primary *Y* axis and in cgs units (cal cm^{-1} s^{-1} K^{-1}) on the secondary *Y* axis. The thermal conductivity values for the cemented and uncemented samples are also presented in Table 2, along with the initial temperature and power applied across the heating wire for each measurement. Thermal conductivity data and experimental conditions for the glass beads used in comparison were published in Appendix C of *Presley* [1995].

1.1 g · kg^{-1} should be roughly equivalent to ~0.1% salt by volume. This laboratory result is consistent with the thermal conductivity increase predicted by *Piqueux and Christensen* [2009] for low salt concentrations. This correspondence is quite reasonable considering the relatively low salt concentration and the disrupted cement bonds of the sample.

Table 2. Thermal Conductivity of the "Cemented" and "Uncemented" Samples

Atmospheric Pressure (torr)	Initial Temperature (°C)	Power (W/m)	Thermal Conductivity (W/m K)
A1A "cemented" sample			
0.5	22.1	0.5823	0.0260
1.0	22.8	0.5499	0.0414
2.0	22.2	0.5419	0.0519
3.0	22.8	0.5286	0.0619
4.0	22.1	0.5572	0.0661
5.0	21.6	0.5582	0.0778
6.0	22.3	0.5263	0.0795
7.0	22.5	0.5216	0.0908
8.0	22.6	0.5260	0.0958
9.0	23.5	0.5196	0.112
10.0	21.3	0.5501	0.113
12.0	23.3	0.5215	0.118
15.0	23.6	0.5188	0.115
A1B "uncemented" sample			
0.6	21.0	0.6161	0.00702
1.0	22.0	0.5898	0.0101
2.0	21.1	0.5610	0.0162
3.0	21.1	0.4905	0.0216
4.0	21.8	0.5459	0.0258
5.0	21.8	0.4850	0.0291
6.0	21.3	0.4801	0.0314
7.0	21.6	0.5380	0.0342
8.0	21.3	0.5362	0.0394
9.0	21.3	0.5365	0.0382
10.0	21.6	0.5938	0.0389
12.0	21.0	0.5955	0.0461
15.0	22.4	0.5305	0.0499
20.0	21.0	0.5894	0.0557

[37] The limitations of this experiment illuminate some of the problems associated with measuring thermal conductivities of salt-cemented particulates, as discussed in section 1. Remote measurement of temperature response is one way to avoid these problems both in situ and in the lab. A new thermal conductivity laboratory that will utilize a Forward-Looking Infrared (FLIR) camera and an environmental chamber capable of Martian atmospheric pressures and temperatures has been constructed at the Mars Space Flight Facility at Arizona State University. At this point, there is no ideal laboratory or field technique to measure thermal conductivity, particularly of salt encrusted particulates. However, since the cement bonds will not be broken in the process of sampling or measurement, FLIR-type instruments hold a promising potential for future work on salt encrusted particulates. As other thermal conductivity laboratories capable of analysis under Martian atmospheric conditions are designed [e.g., *Hütter et al.*, 2008], efforts should be made to establish a "standard" sample, so that results between laboratories may be adequately compared, and to encourage better quality results. Thermal modeling should increasingly be used in tandem with laboratory and field measurements, so that we may understand better the properties that control thermal conductivity, as well as to establish a more detailed understanding of the limitations of the techniques that we utilize for measurement and of those models.

[38] **Acknowledgments.** We appreciate the very thoughtful reviews from Michael Mellon and an anonymous reviewer, as well as additional comments from Robert Carlson and Nathan Putzig. These suggestions allowed us to significantly improve the manuscript. We are grateful to Evert Fruitman and Bill Coleman for upgrades and repairs to the signal conditioner; to Rossman Irwin, Ruslan Kusmin, and Ted Maxwell for their help

collecting the Australian samples in the field; to Bryan MacFarlane for particle size analysis; to Everett Schock for use of the GEOPIG Ion Analysis Laboratory; to Tracy Lund for running the sample, duplicates, and blanks through the ion chromatograph columns; and to Phil Christensen for support of the Thermal Conductivity laboratory at Arizona State University. The Smithsonian Institution provided the funds for the purchase and transport of the Troxler 3450 moisture density gauge and for the operator license. This study was primarily supported by NASA grant NAG5-12180, with additional funding from grant NAG5-10214.

References

Abu-Hamdeh, N. H., and R. C. Reeder (2000), Effects of density, moisture, salt concentration, and organic matter, *Soil Sci. Soc. Am. J.*, *64*, 1285–1290.

Arvidson, R. E., E. A. Guinness, M. A. Dale-Bannister, J. Adams, M. Smith, P. R. Christensen, and R. B. Singer (1989), Nature and distribution of surficial deposits in Chryse Planitia and vicinity, Mars, *J. Geophys. Res.*, *94*(B2), 1573–1587.

Baird, A. K., P. Toulmin III, B. C. Clark, H. J. Rose Jr., K. Keil, R. P. Christian, and J. L. Gooding (1976), Mineralogic and petrologic implications of Viking geochemical results from Mars: Interim report, *Science*, *194*(4271), 1288–1293.

Binder, A. B., R. E. Arvidson, E. A. Guinness, K. L. Jones, E. C. Morris, T. A. Mutch, D. C. Pieri, and C. Sagan (1977), The geology of the Viking Lander 1 site, *J. Geophys. Res.*, *82*(28), 4439–4451.

Bishop, J. L., and E. Murad (2005), The visible and infrared spectral properties of jarosite and alunite, *Am. Mineral.*, *90*(7), 1100–1107.

Bourke, M. C., and G. Pickup (1999), Fluvial form variability in arid central Australia, in *Varieties of Fluvial Form*, edited by A. J. Miller and A. Gupta, pp. 249–271, Wiley, Hoboken, N. J.

Burns, R. G. (1986), Terrestrial analogues of the surface rocks of Mars?, *Nature*, *320*, 55–56.

Burns, R. G. (1987), Ferric sulfates on Mars, *J. Geophys. Res.*, *92*(12), E570–E574.

Burns, R. G. (1988), Gossans on Mars, in *Proc. Lunar Planet. Sci. 18th*, pp. 713–721, Cambridge Univ. Press/Lunar and Planetary Inst., Houston, Tex.

Burns, R. G. (1993), Rates and mechanisms of chemical weathering of ferromagnesium silicate minerals on Mars, *Geochim. Cosmochim. Acta*, *57*(19), 4555–4574.

Burns, R. G., and D. S. Fisher (1990), Iron-sulfur mineralogy of Mars: Magmatic evolution and chemical weathering products, *J. Geophys. Res.*, *95*(B9), 14,415–14,421.

Buurman, P., B. van Lagen, and E. J. Velthorst (1996), *Manual for Soil and Water Analysis*, 314 pp., Backhuys Publishers, Leiden, Netherlands.

Christensen, P. R., and H. J. Moore (1992), The Martian surface layer, in *Mars*, edited by H. H. Kieffer et al., pp. 686–729, Univ. of Arizona Press, Tucson, Ariz.

Christensen, P. R., et al. (2004), Mineralogy at Meridiani Planum from the mini-TES experiment on the Opportunity rover, *Science*, *306*(5702), 1733–1739.

Clark, B. C., A. K. Baird, H. J. Rose Jr., P. Toulmin III, K. Keil, A. J. Castro, W. C. Kelliher, C. D. Rowe, and P. H. Evans (1976), Inorganic analyses of Martian surface samples at the Viking Landing sites, *Science*, *194*(4271), 1283–1288.

Cremers, C. J. (1971), A thermal conductivity cell for small powdered samples, *Rev. Sci. Instrum.*, *42*(11), 1694–1696.

DeVries, D. A. (1952), The thermal conductivity of soil, *Meded. Landbouwhogesch. Wageningen*, *52*(1), 1–73. (Translated by Building Research Station (Library Communication No. 759), U. K.)

Fergason, R. L., P. R. Christensen, J. F. Bell III, M. P. Golombek, K. E. Herkenhoff, and H. H. Kieffer (2006), Physical properties of the Mars Exploration Rover landing sites as inferred from Mini-TES-derived thermal inertia, *J. Geophys. Res.*, *111*, E02S21, doi:10.1029/2005JE002583.

Fountain, J. A., and E. A. West (1970), Thermal conductivity of particulate basalt as a function of density in simulated lunar and Martian environments, *J. Geophys. Res.*, *75*(20), 4063–4069.

Gellert, R., et al. (2004), Chemistry of rocks and soils in Gusev Crater from the Alpha Particle X-ray Spectrometer, *Science*, *305*(5685), 829–832.

Goodall, T. M., C. P. North, and K. W. Glennie (2000), Surface and subsurface sedimentary structures produced by salt crusts, *Sedimentology*, *47*, 99–118.

Hollands, C. B., G. C. Nanson, B. G. Jones, C. S. Bristow, D. M. Price, and T. J. Pietcsch (2006), Aeolian-fluvial interaction: Evidence for Late Quaternary channel change and wind-rift linear dune formation in the northwestern Simpson Desert, Australia, *Quat. Sci. Rev.*, *25*(1–2), 142–162.

Hunt, G. R., J. W. Salisbury, and C. J. Lenhoff (1971), Visible and near-infrared spectra of minerals and rocks: IV. Sulphides and sulphates, *Modern Geol.*, *3*, 1–14.

Hunter, K. A., D. S. Mackie, P. W. Boyd, and G. H. McTainsh (2006), From desert to dessert: Why Australian dust matters, *EOS Trans.*, *AGU*, Fall Meet. Suppl., Abstract A42C-03.

Hütter, E. S., N. I. Koemle, G. Kargl, and E. Kaufmann (2008), Determination of the effective thermal conductivity of granular materials under varying pressure conditions, *J. Geophys. Res.*, *113*, E12004, doi:10.1029/2008JE003085.

Hynek, B. M., and K. Singer (2007), Ground truth from the Opportunity Rover for Mars thermal inertia data, *Geophys. Res. Lett.*, *34*, L11201, doi:10.1029/2007GL029687.

Iversen, J. D., and B. R. White (1982), Saltation threshold on Earth, Mars and Venus, *Sedimentology*, *29*, 111–119.

Jakosky, B. M., and P. R. Christensen (1986), Global duricrust on Mars: Analysis of remote-sensing data, *J. Geophys. Res.*, *91*(B3), 3547–3559.

Johansen, O. (1975), Thermal conductivity of soils, Ph.D. Thesis, Trondheim, Norway, (CRREL Draft Translation 637, 1977), ADA 044002.

Kieffer, H. H., P. A. Davis, and L. A. Soderblom (1981), Mars' global properties: Maps and applications, *Proc. Lunar Planet. Conf.*, *12B*, 1395–1417.

Klingelhöfer, G., et al. (2004), Jarosite and hematite at Meridiani Planum from Opportunity's Mössbauer Spectrometer, *Science*, *306*(5702), 1740–1745.

Lindsay, J. F. (1987), Upper proterozoic evaporates in the Amadeus basin, central Australia, and their role in basin tectonics, *GSA Bull.*, *99*(6), 852–865.

Mellon, M. T., B. M. Jakosky, and S. E. Postawko (1997), The persistence of equatorial ground ice on Mars, *J. Geophys. Res.*, *102*(E8), 19,357–19,369.

Mellon, M. T., B. M. Jakosky, H. H. Kieffer, and P. R. Christensen (2000), High-resolution thermal inertia mapping from the Mars Global Surveyor Thermal Emission Spectrometer, *Icarus*, *148*, 437–455.

Mellon, M. T., R. L. Fergason, and N. E. Putzig (2008), The thermal inertia of the surface of Mars, in *The Martian Surface: Composition, Mineralogy, and Physical Properties*, edited by J. W. Bell, pp. 399–427, Cambridge Univ. Press, Cambridge, U. K.

Merényi, E., K. S. Edgett, and R. B. Singer (1996), Deucalionis Regio, Mars: Evidence for a new type of immobile weathered soil unit, *Icarus*, *124*, 296–307.

Midttømme, K., J. Saettem, and E. Roaldset (1997), Thermal conductivity of unconsolidated sediments from the Vøring Basin, Norwegian Sea, *Nord. Petrol. Technol. Ser. II*, 145–197.

Moore, H. J., D. B. Bickler, J. A. Crisp, H. J. Eisen, J. A. Gensler, A. F. C. Haldemann, J. R. Matijevic, L. K. Reid, and F. Pavlics (1999), Soil-like deposits observed by Sojourner, the Pathfinder rover, *J. Geophys. Res.*, *104*(E4), 8729–8746.

Morris, R. V., et al. (2006), Mössbauer mineralogy of rock, soil, and dust at Meridiani Planum, Mars: Opportunity's journey across sulfate-rich outcrop, basaltic sand and dust, and hematite lag deposits, *J. Geophys. Res.*, *111*, E12S15, doi:10.1029/2006JE002791.

Mutch, T. A., et al. (1976), The surface of Mars: The view from the Viking 2 lander, *Science*, *194*(4271), 1277–1283.

Piqueux, S. and P. R. Christensen (2009), A model of thermal conductivity for planetary soils: 2. Theory for cemented soils, *J. Geophys. Res.*, *114*, E09006, doi:10.1029/2008JE003309.

Presley, M. A. (1995), Thermal conductivity measurements of particulate materials: Implications for surficial units on Mars, Ph.D. Dissertation, Ariz. State Univ., Tempe.

Presley, M. A., and R. E. Arvidson (1988), Nature and origin of materials exposed in the Oxia Palus-Western Arabia-Sinus Meridiani region, Mars, *Icarus*, *75*, 499–517.

Presley, M. A., and P. R. Christensen (1997), Thermal conductivity measurements of particulate materials: 2. Results, *J. Geophys. Res.*, *102*(E3), 6551–6566.

Presley, M. A., and R. A. Craddock (2006), Thermal conductivity measurements of particulate materials: 3. Natural samples and mixtures of particle sizes, *J. Geophys. Res.*, *111*, E09013, doi:10.1029/2006JE002706.

Putzig, N. E., M. T. Mellon, K. A. Kretke, and R. E. Arvidson (2005), Global thermal inertia and surface properties of Mars from the MGS mapping mission, *Icarus*, *173*, 325–341.

Rieder, R., T. Economou, H. Wänke, A. Turkevich, J. Crisp, J. Brückner, G. Dreibus, and H. Y. McSween Jr. (1997), The chemical composition of Martian soil and rocks returned by the mobile Alpha Proton X-ray Spectrometer: Preliminary results from the X-ray mode, *Science*, *278*(5344), 1771–1774.

Schofield, R., D. S. G. Thomas, and M. J. Kirkby (2001), Causal processes of soil salinization in Tunisia, Spain and Hungary, *Land Degrad. Develop.*, *12*, 163–181.

Seiferlin, K., M. Heimberg, and N. Thomas (2007), The effect of soil cementation on the thermal conductivity, *Geophys. Res. Abstr.*, *9*, EGU2007-A-02361.

Smoluchowski, M. M. (1910), Sur la conductibilite calorifique des corps pulverizes, *Bull. Int. Acad. Sci. Cacovie*, *5A*, 129–153.

Squyres, S. W., et al. (2004), In-situ evidence for an ancient aqueous environment at Meridiani Planum, Mars, *Science*, *306*(5702), 1709–1714.

U.S. Salinity Laboratory Staff (1954), chap. 6, Methods for soil characterization in *Diagnosis and Improvement of Saline and Alkali Soils*, edited by L. A. Richards, *Agriculture Handbook 60,* 83-126, USDA, Washington, D. C.

Van Rooyen, M., and H. G. Winterkorn (1959), Structural and textural influences on thermal conductivity of soils, *Highw. Res. Board Proc.*, *39*, 576–621.

Wang, A., et al. (2006), Sulfate deposition in subsurface regolith in Gusev Crater, Mars, *J. Geophys. Res.*, *111*, E02S17, doi:10.1029/2005JE002513.

Wechsler, A. E., and P. E. Glaser (1965), Pressure effects on postulated lunar materials, *Icarus*, *4*, 335–352.

Williams, G. E. (1971), Flood deposits of the sand-bed ephemeral streams of central Austrialia, *Sedimentology*, *17*(1/2), 1–40.

R. A. Craddock, Center for Earth and Planetary Studies, National Air and Space Museum, Smithsonian Institution, 6th Street and Independence Avenue, S. W., Washington, DC 20560-0315, USA.

M. A. Presley, School of Earth and Space Exploration, Mars Space Flight Facility, Arizona State University, Box 876305, Tempe, AZ 85287-6305, USA. (swmartian@fastmail.fm)

N. Zolotova, School of Earth and Space Exploration, Arizona State University, Box 871404, Tempe, AZ 85287-1404, USA.